



Molecular Physics

An International Journal at the Interface Between Chemistry and Physics

ISSN: 0026-8976 (Print) 1362-3028 (Online) Journal homepage: <http://www.tandfonline.com/loi/tmph20>

Unravelling open-system quantum dynamics of non-interacting Fermions

Zhu Ruan & Roi Baer

To cite this article: Zhu Ruan & Roi Baer (2018): Unravelling open-system quantum dynamics of non-interacting Fermions, Molecular Physics, DOI: [10.1080/00268976.2018.1456685](https://doi.org/10.1080/00268976.2018.1456685)

To link to this article: <https://doi.org/10.1080/00268976.2018.1456685>



Published online: 19 Apr 2018.



Submit your article to this journal [↗](#)



Article views: 6



View related articles [↗](#)



View Crossmark data [↗](#)

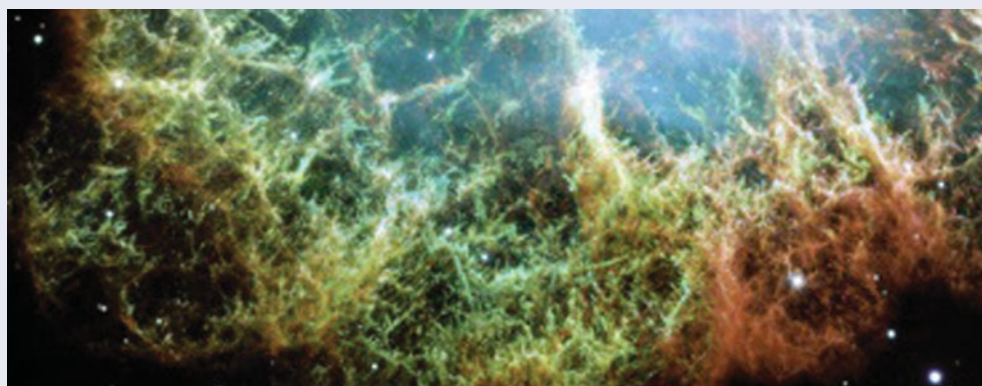
Unravelling open-system quantum dynamics of non-interacting Fermions

Zhu Ruan and Roi Baer

Fritz Haber Center for Molecular Dynamics, Institute of Chemistry, The Hebrew University of Jerusalem, Jerusalem, Israel

ABSTRACT

The Lindblad equation is commonly used for studying quantum dynamics in open systems that cannot be completely isolated from an environment, relevant to a broad variety of research fields, such as atomic physics, materials science, quantum biology and quantum information and computing. For electrons in condensed matter systems, the Lindblad dynamics is intractable even if their mutual Coulomb repulsion could somehow be switched off. This is because they would still be able to affect each other by interacting with the bath. Here, we develop an approximate approach, based on the Hubbard–Stratonovich transformation, which allows to evolve non-interacting Fermions in open quantum systems. We discuss several applications for systems of trapped 1D Fermions showing promising results.



ARTICLE HISTORY

Received 11 February 2018
Accepted 13 March 2018

KEYWORDS

Lindblad equations; density matrix; open quantum systems; open fermion system

1. Introduction

Decoherence, dephasing and dissipation in large open quantum systems are important phenomena in a broad variety of fields, such as nonadiabatic processes in chemistry and materials science, [1–7], quantum biology [8,9] and quantum information [10,11]. They are commonly described using the concept of the density matrix (DM), which generalises the notion of a wave function as the quantum state descriptor. Despite great success in atomic physics, DM approaches have not found extensive application in the field of large electronic systems, except in cases of small systems, where it is sufficient and possible to address only a small number of electronic states [12–18]. For describing the quantum dynamics of open systems having a large number of electrons and electronic states a different approach is probably needed. Here, it is natural to consider time-dependent (current) density functional theory (TDDFT), based on the Runge–Gross

(RG) theorem [19] which simplifies the treatment of the dynamics of interacting electrons by mapping them onto non-interacting Fermions. Extensions of the RG theorem to open systems have indeed appeared [20–25], but the follow-up progress has yet to be achieved, and the main cause for delay is the fact that non-interacting Fermions develop an interaction through the coupling with the bath.¹

In this paper, we develop a method to describe the DM time evolution of non-interacting Fermions (Section 2) as they are coupled to an external bath. We work within the Lindblad formalism [26–29], which is useful for describing Markovian open system dynamics. The method makes use of the unravelling procedure, which transforms the Lindblad equation on the DM into a random walk in wave functions space. The effective Fermion–Fermion interactions induced by the bath are converted into *additional* random-walk terms. Applications of the method, first to an analytically solvable model

and then to a system of trapped 1D Fermions in a double-well are given in Section 3. We believe that the present development forms a significant stepping stone for applying TDDFT to the study of the dynamics of open electronic systems in the future.

2. Fermion unravelling

DM operator $\hat{\rho}$ represents the quantum state of a system, open or closed, generalising the concept of a pure wave function. It can be written in terms of its eigenvalues w_s and eigenfunctions Φ^s as

$$\hat{\rho}(t) = \sum_s p_s(t) |\Phi^s(t)\rangle\langle\Phi^s(t)| \quad (1)$$

and the eigenvalues $p_s(t)$ being the probability for the system to be in state Φ^s . Clearly, the DM must be Hermitian, positive-definite ($p_s(t) > 0$) and unit-traced ($\sum_s p_s(t) = 1$). If \hat{O} is an operator corresponding to an observable property, then the expectation value of its measurement is expressed neatly as a trace: $O(t) = \text{tr}[\hat{\rho}(t)\hat{O}] = \sum_s p_s(t)\langle\Phi^s(t)|\hat{O}|\Phi^s(t)\rangle$. In any time-dependent process, the DM evolution is determined by an equation of motion which must preserve its trace, its Hermiticity and its positivity. The most general ‘Markovian’ equation of motion that respects these basic tenants is the so-called Lindblad-equation [26,28–30]:

$$\dot{\hat{\rho}}(t) = -\frac{i}{\hbar} [\hat{H}, \hat{\rho}] + \mathfrak{D}\hat{\rho}(t), \quad (2)$$

where $\hat{H} = \hat{H}^\dagger$ is the Hermitian *effective Hamiltonian* and the *dissipative* part, which is of the form:

$$\mathfrak{D}\hat{\rho} = \left(\hat{L}^\alpha \hat{\rho} \hat{L}^{\alpha\dagger} - \frac{1}{2} \hat{L}^{\alpha\dagger} \hat{L}^\alpha \hat{\rho} - \frac{1}{2} \hat{\rho} \hat{L}^{\alpha\dagger} \hat{L}^\alpha \right), \quad (3)$$

where \hat{L}^α are *Lindblad operators* ($\alpha = 1, 2, \dots, N_L$ and we adopt the Einstein convention that repeated dummy indices get summed). These equations of motions are supplemented by an initial condition $\rho_s(0)$ and $\Phi_s(0) = \Phi_0^s$ at $t = 0$.

For many-body systems, working with the DM is difficult, if not impossible and therefore unravelling procedures [31–34] were developed where the DM is represented as an expected value involving *random* wave functions $\Phi(t)$

$$\hat{\rho}(t) = E \left\{ \frac{|\Phi(t)\rangle\langle\Phi(t)|}{\langle\Phi(t)|\Phi(t)\rangle} \right\}. \quad (4)$$

In each of these states, $\Phi(t)$ start from a randomly selected initial state Φ_0^s with probability $\rho_s(0)$ and is then evolved separately in time according to the following non-linear

stochastic Schrödinger equation:

$$d\Phi(t) = \left[-\frac{i}{\hbar} \hat{H} dt + \left(\langle L^\alpha \rangle_t^* - \frac{1}{2} \hat{L}^{\alpha\dagger} \right) dt + d\omega_\alpha \right] \hat{L}^\alpha \Phi(t), \quad (5)$$

where $d\omega_\alpha$ are independent Wiener processes with $E[d\omega^\alpha d\omega^\beta] = \delta^{\alpha\beta} dt$ and $\langle L^\alpha \rangle_t \equiv \frac{\langle\Phi(t)|\hat{L}^\alpha|\Phi(t)\rangle}{\langle\Phi(t)|\Phi(t)\rangle}$ [34] or $\langle L^\alpha \rangle_t = \frac{\text{Re}\langle\Phi(t)|\hat{L}^\alpha|\Phi(t)\rangle}{\langle\Phi(t)|\Phi(t)\rangle}$ [32]. This equation is much easier to handle than Equation (2) since it involves only the wave function. But this comes with a sizable price tag: a non-linear Schrödinger equation combined with stochastic noise.

The unravelling procedure given above applies to all Lindblad equations, in particular for non-interacting Fermion systems, where the effective Hamiltonian and the Lindblad operators are one-body operators:

$$\hat{H} = \sum_n \hat{h}(n), \quad (6)$$

$$\hat{L}^\alpha = \sum_n \hat{\ell}^\alpha(n), \quad (7)$$

where

$$\hat{h} = \frac{\hat{p}^2}{2m} + V(\hat{x}) \quad (8)$$

is a single electron Hamiltonian ($\hat{h}(n)$ is this Hamiltonian applied for electron number n). One notices that the term $\hat{L}^{\alpha\dagger}\hat{L}^\alpha = \sum_{mm} \hat{\ell}^{\alpha\dagger}(n)\hat{\ell}^\alpha(m)$ appearing in Equation (5) is a two-body operator and thus the unravelling of non-interacting electrons is essentially an interacting electron problem.

We make progress here through the Hubbard–Stratonovich (HS) transformation [35,36], $e^{-\frac{1}{2}\hat{R}^2 dt} \propto \int_{-\infty}^{\infty} e^{-\frac{\eta^2}{2dt}} e^{i\hat{R}\eta} d\eta$ which converts Equation (5) into a new equation involving a three-component Brownian (Wiener) motion

$$d\Phi(t) = -\frac{i}{\hbar} \left(\hat{H} dt - i \left(d\hat{H}_R + d\hat{H}_C + d\hat{H}_S \right) \right) \Phi(t), \quad (9)$$

where

$$d\hat{H}_R \equiv -\hbar [\langle L^\alpha \rangle_t^* dt + d\omega_\alpha + idu_\alpha] \hat{R}^\alpha, \quad (10)$$

$$d\hat{H}_S \equiv -\hbar [\langle L^\alpha \rangle_t^* dt + d\omega_\alpha + dv_\alpha] i\hat{S}^\alpha, \quad (11)$$

$$d\hat{H}_C \equiv \hbar \sum_\alpha \hat{C}^\alpha dt, \quad (12)$$

where $\hat{R}^\alpha = \text{Re}[\hat{L}^\alpha]$, $\hat{S}^\alpha = \text{Im}[\hat{L}^\alpha]$ and $\hat{C}^\alpha = i[\hat{R}^\alpha, \hat{S}^\alpha]$ are three Hermitian one-particle operators (so that $\hat{L}^{\alpha\dagger}\hat{L}^\alpha =$

$\hat{R}^\alpha \hat{R}^\alpha + \hat{S}^\alpha \hat{S}^\alpha + \hat{C}$) and where like dw_α , also du_α , dv_α are each a Wiener process i.e. a random number drawn from the normal distribution with mean zero and variance dt . There is, however, an important, a delicate, point here. For each dw_α , we must sample du_α and dv_α many times so as to enable an accurate calculation of $\langle L^\alpha \rangle_t$. Hence, the algorithm we use to evolve the DM of non-interacting Fermions is as follows:

- (1) Assume we have the Slater wave function $\Phi(t) = \det[\phi_1(t) \cdots \phi_N(t)]$ and the expected values $L^\alpha(t)$.
- (2) Propagate from $t \rightarrow t + dt$:
 - (a) Sample dw_α .
 - (b) Holding dw_α fixed, we sample du_α and $dv_\alpha N_{\text{HS}}$ times and for each pair of such values we propagate in time $\Phi(t)$ to a new Slater wave-function $\Phi^{(k)}(t + \Delta t) = \det[\phi_1^{(k)}(x_1) \cdots \phi_N^{(k)}(x_N)]$

$$\phi_n^{(k)}(t + \Delta t) = e^{-\frac{i}{\hbar}(\hat{h}dt - i(d\hat{h}_R + d\hat{h}_C + d\hat{h}_S))} \phi_n(t) \quad (13)$$

for $k = 1, \dots, N_{\text{HS}}$.

- (c) Generate from $\Phi^{(1)}, \dots, \Phi^{(N_{\text{HS}})}$ the one-particle DM $\rho_1(r, r')$ and diagonalise it:

$$\rho_1(r, r') = \sum_n \tilde{p}_n \tilde{\phi}_n(r) \tilde{\phi}_n(r')^*, \quad (14)$$

(where $\tilde{p}_1 \geq \tilde{p}_2 \geq \tilde{p}_3 \dots$). Now, select the first eigenfunctions $\tilde{\phi}_n$ of ρ_1 and form from them the Slater wave function to be used as the wave function for the next time step $\Phi(t + dt) \equiv \det[\tilde{\phi}_1 \cdots \tilde{\phi}_N]$. We note that $\Phi(t + dt)$ is the single determinant wave function which reproduces the one-body DM ρ_1 as close as possible. The initial state and the expected values for the Lindblad operator to be used in the next iteration will thus be calculated as

$$\langle L^\alpha \rangle_{t+dt} = \sum_{n=1}^N \langle \tilde{\phi}_n | \hat{L}^\alpha | \tilde{\phi}_n \rangle. \quad (15)$$

The last step of the algorithm involves collapsing the HS step into a Slater wave function having a similar one-body DM. This step can be generalised and one can retain an ensemble of $Q \geq 1$ Slater wave functions that yield a similar one-body DM. We should check that the calculation is converged with respect to Q . In the present paper, we do not attempt to converge the calculation results with respect to Q . In many applications, the system is automatically driven to its thermal equilibrium state

which is an eigenstate of the non-interacting Hamiltonian \hat{H} , i.e. an ensemble of Slater wave functions.

3. Applications to trapped 1D Fermions

To demonstrate the validity of the method, we report calculations on systems of N non-interacting spin-up Fermions of mass $m = 1m_e$ (atomic units are used in all reported numerical results) trapped in a 1D potential $V(x)$ (see Equation (8)) and using only one Lindblad operator

$$\hat{\ell} \equiv \sqrt{\frac{m\omega_\ell\gamma}{2\hbar N}} \left(\hat{x} + \frac{i}{m\omega_\ell} \hat{p} \right) \quad (16)$$

to be used in Equation (7). Note that $\hat{\ell}$ is the lowering ladder operator for a harmonic oscillator of frequency ω_ℓ (although it is still a Fermionic operator). In the results shown below, we use $\omega_\ell = 1E_h/\hbar$ and $\gamma = 0.2E_h/\hbar$ and $N = 8$ Fermions. The calculation was carried out using a high-order numerical implementation of the algorithm depicted in the previous section, where the single particle wave functions and operators were represented on a Fourier grid and the non-unitary time propagation was performed using a high-degree interpolating polynomial in the Newton form [37,38].

3.1. Validation: Fermions in a harmonic trap

To demonstrate the validity of the method, we apply it to a system of $N = 8$ Fermions having the Hamiltonian of Equation (8) with a Harmonic potential

$$V(x) = \frac{1}{2}m\omega^2 x^2, \quad (17)$$

$$\omega = \omega_\ell = 1E_h/\hbar.$$

In this case, the expectation values of the total displacement $X_t = \langle \sum_{n=1}^N \hat{x}_n \rangle_t$ and total momentum $P_t = \langle \sum_{n=1}^N \hat{p}_n \rangle_t$ can be determined analytically directly from the Lindblad equation:

$$X_t^{an} = (P_0 \cos \omega t + \frac{P_0}{m\omega} \sin \omega t) e^{-\frac{\gamma}{2}t}, \quad (18)$$

$$P_t^{an} = (P_0 \cos \omega t - m\omega X_0 \sin \omega t) e^{-\frac{\gamma}{2}t}. \quad (19)$$

These trajectories are dependent only on the initial values of the total displacement X_0 and momentum P_0 and not explicitly on the number of electrons N or on other properties of the initial state. In our demonstration, we start from a pure state which is taken as the a

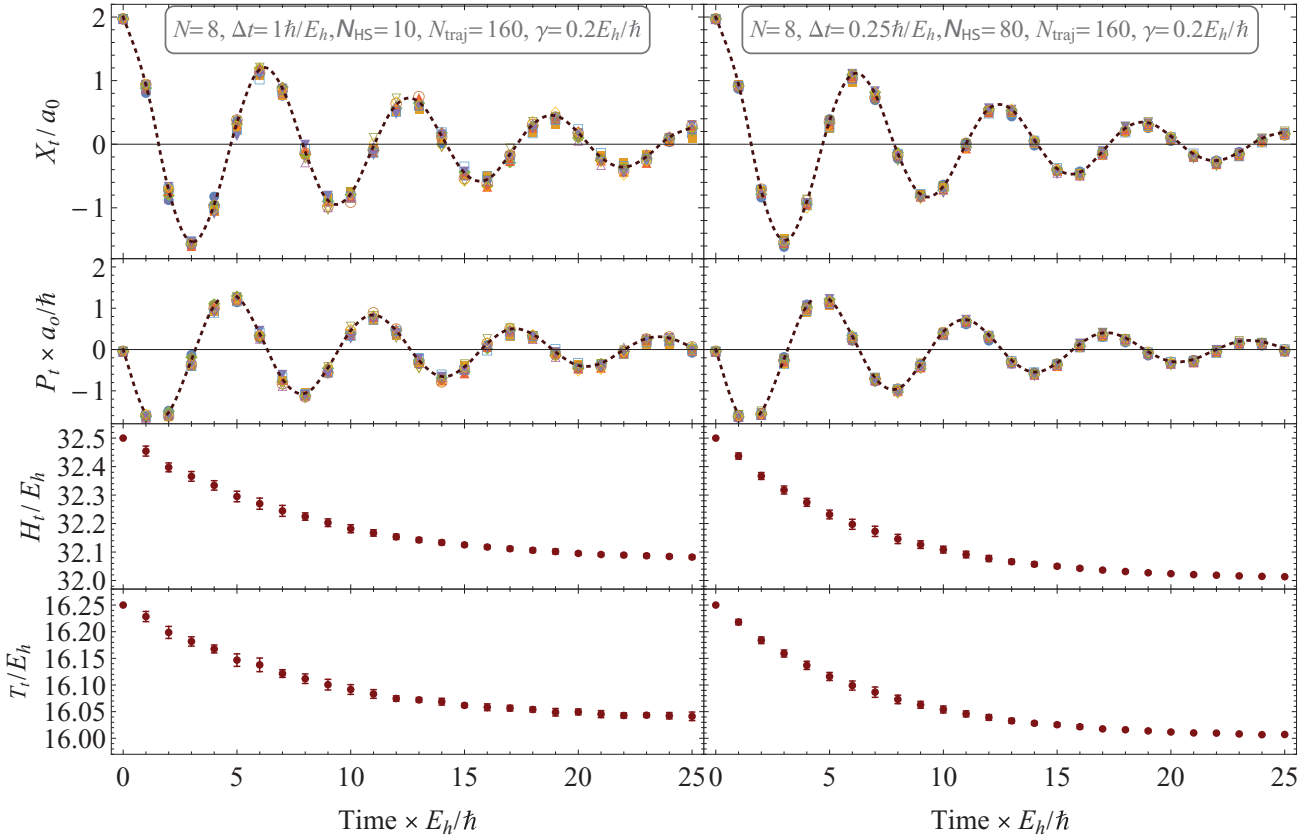


Figure 1. The time-dependent total displacement X_t , total momentum P_t , total energy H_t and total kinetic energy T_t transients for eight non-interacting Fermions in the Harmonic trap of Section 3.1, starting from the pure state $\hat{\rho}_\theta = |\Phi_\theta\rangle\langle\Phi_\theta|$ with $\theta = \pi/4$. The X_t and P_t panels show analytical transients (Equation (18)) as dashed lines while the calculated results of 10 independent runs (each having 160 trajectories) are shown as symbols. The H_t and T_t results are depicted as statistical error bars centred on the average over the 10 runs. The computed results shown in the left and right panels are based on different time steps Δt and the number of HS iterations N_{HS} .

non-stationary Slater wave-function

$$\Phi_\theta = \frac{1}{N!} \det [\psi_1(x_1) \cdots \psi_{N-1}(x_{N-1}) \varphi_\theta(x_N)], \quad (20)$$

where $\{\psi_n(x)\}_{n=1}^{N+1}$ are the $N+1$ lowest energy single-particle eigenstates (so-called molecular orbitals (MO)) of \hat{h} , and

$$\varphi_\theta(x) = \psi_N(x) \cos \theta + \psi_{N+1}(x) \sin \theta \quad (21)$$

is a linear combination involving the highest occupied MO (HOMO) $\psi_N(x)$ and the lowest unoccupied MO (LUMO) $\psi_{N+1}(x)$. The angle θ is taken as $\pi/4$, expressing an equal weight of these two orbitals.

In Figure 1, we show the analytical trajectory and the results of 10 independent runs, each based on $N_{\text{traj}} = 160$ trajectories. The results in the left panel use a time step of $\Delta t = 1\hbar/E_h$ each employing $N_{\text{HS}} = 10$ HS iterations while in the right panel $\Delta t = 0.25\hbar/E_h$ and $N_{\text{HS}} = 80$. It can be seen that the numerical results follow closely the analytical trajectories, with somewhat improved performance for the smaller time step and more

intensive HS sampling. The total and kinetic energies for the trajectories decay to a finite value as t grows. The asymptotic values for the total and kinetic energies are pushed closer to their ground state values (which, for this system are $E = 32E_h$ and $T = 16E_h$, respectively) as we reduce Δt and increase the number of HS iterations.

A closer look into the accuracy of the dynamics is given in Figure 2, where the 75% confidence intervals (CIs) for the difference $X_t - X_t^{\text{an}}$ are given at two times, namely $t = 23\hbar/E_h$ and $t = 25\hbar/E_h$ as a function of N_{HS} and for two time-steps Δt . For $N_{\text{HS}} < 8$, the results show explicit bias since the error bars of $N_{\text{HS}} \geq 8$ are almost non-overlapping with those of $N_{\text{HS}} < 8$. For $N_{\text{HS}} > 8$, the main effect of N_{HS} is reduction of the error bars (namely improved sampling removes noise). Even for $N_{\text{HS}} > 8$, the CIs do not include the exact result ($X_t - X_t^{\text{an}} = 0$) showing that a bias exists due to another source, namely the time-step error. Indeed, as Δt decreases from 1 to 0.25 this bias decreases by this bias decreases substantially. From this, we conclude that the total error is dominated by the finite time-step approximation once $N_{\text{HS}} \geq 8$.

Note, however, that the correct value, namely $X_t - X_t^{\text{an}} = 0$, will not be included in the CIs when we increase

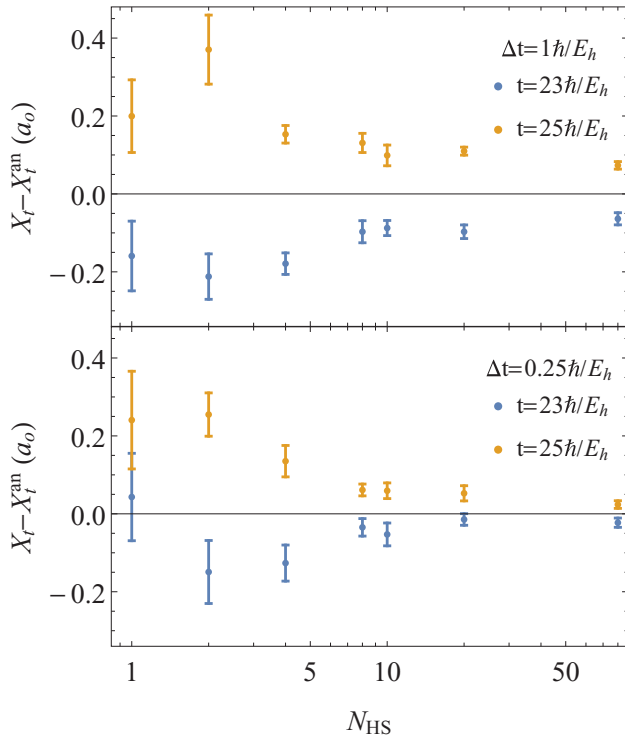


Figure 2. 75% confidence intervals for the difference between the estimated and analytical displacements at two different values of t as a function of the number N_{HS} of HS iterations, for the harmonic system of Section 3.1. Two time steps are considered: $\Delta t = 1\hbar/E_h$ (top panel) and $\Delta t = 0.25\hbar/E_h$ (bottom panel). The confidence intervals are based on the calculated results from 10 independent runs each having $N_{\text{traj}} = 160$ trajectories.

N_{traj} due to the finite- N_{HS} and finite- Δt errors which are clearly noticeable and which can be systematically reduced by increasing N_{HS} and by diminishing Δt . The results seem converged with respect to N_{HS} once $N_{\text{HS}} > 10$ (i.e. although increasing N_{HS} lowers the fluctuation, it does not change the average), on the other hand, the main source of bias is the size of the time step.

3.2. A double-well trap

As an application of the method, we study $N = 8$ Fermions in a double-well potential obtained by adding to the Harmonic potential of Equation (17) a Gaussian barrier centered at the origin of coordinates:

$$V(x) = \frac{1}{2}m\omega^2 x^2 + V_B e^{-\frac{x^2}{2\sigma_B^2}}, \quad (22)$$

$$V_B = 8E_h, \quad \sigma_B = 0.2a_0.$$

In Figure 3, we study the dynamics under similar conditions of the previous section starting from two different initial pure states $\hat{\rho}_\theta = |\Phi_\theta\rangle\langle\Phi_\theta|$. On the left panel, the initial state ($\theta = \pi/4$) involves a linear

combination of HOMO and LUMO and thus is not an eigenstate of \hat{H} ; therefore a damped oscillation in X and P is observed, which is accompanied by a gradual decrease in the frequency of oscillation. The energy of the system grows in time, as does the kinetic energy, indicating that the bath is *injecting* energy into the system, raising its temperature while at the same time oscillations are damped due to dephasing. On the right panel, we show the transients corresponding to $\theta = \pi/2$, in which the initial state is an excited eigenstate of \hat{H} (where the HOMO is replaced by the LUMO). In an eigenstate there is no motion, so we observe no oscillations in X and T , and it can be supposed that any energy injected by the bath into the system cannot stir up observable oscillation due to the dephasing effects seen in the left panel. The energy here starts, at early times, to decrease but then at $t = 11\hbar/E_h$ it reverses and starts ascending. The kinetic energy follows this trend, indicating a tendency for the temperature to initially drop, reach a minimum somewhat later than the total energy at $t \approx 15\hbar/E_h$ and then rise at later times.

We compare these transients to approximate transients based on the approximation that the population of state i is given by

$$\dot{n}_i(t) = \sum_j [\gamma_{ij}n_j(1-n_i) - \gamma_{ji}n_i(1-n_j)], \quad (23)$$

where $\gamma_{ij} = \sum_\alpha |\ell_{ij}^\alpha|^2$.² The populations n_i enable calculation of the energy and kinetic energy transients shown as dots in Figure 3. Consider first the right panel. Here, the initial DM is diagonal so the dots are close to the stochastic calculation, only deviating significantly when coherences build up at around $t = 5\hbar/E_h$. While the two transients are close only at very early times, they both indicate a non-monotonic behaviour of the energy, first cooling and then heating. For the kinetic energy too there is an agreement at early times where the system cools at first and then heats up. For the left panel, the initial state is not diagonal so the dot transient breaks off from the more accurate calculation almost immediately. Again, both the accurate and the approximate transients agree qualitatively that the system is heated by the bath.

4. Summary

In this paper, we have introduced a new method for treating the dynamics of non-interacting Fermions coupled to an external bath. The main obstacle is the effective inter-particle interactions. We have used the HS transformation for the reformulation of the unravelled dynamics to include several types of random walks (three for each Lindblad operator) which together allow

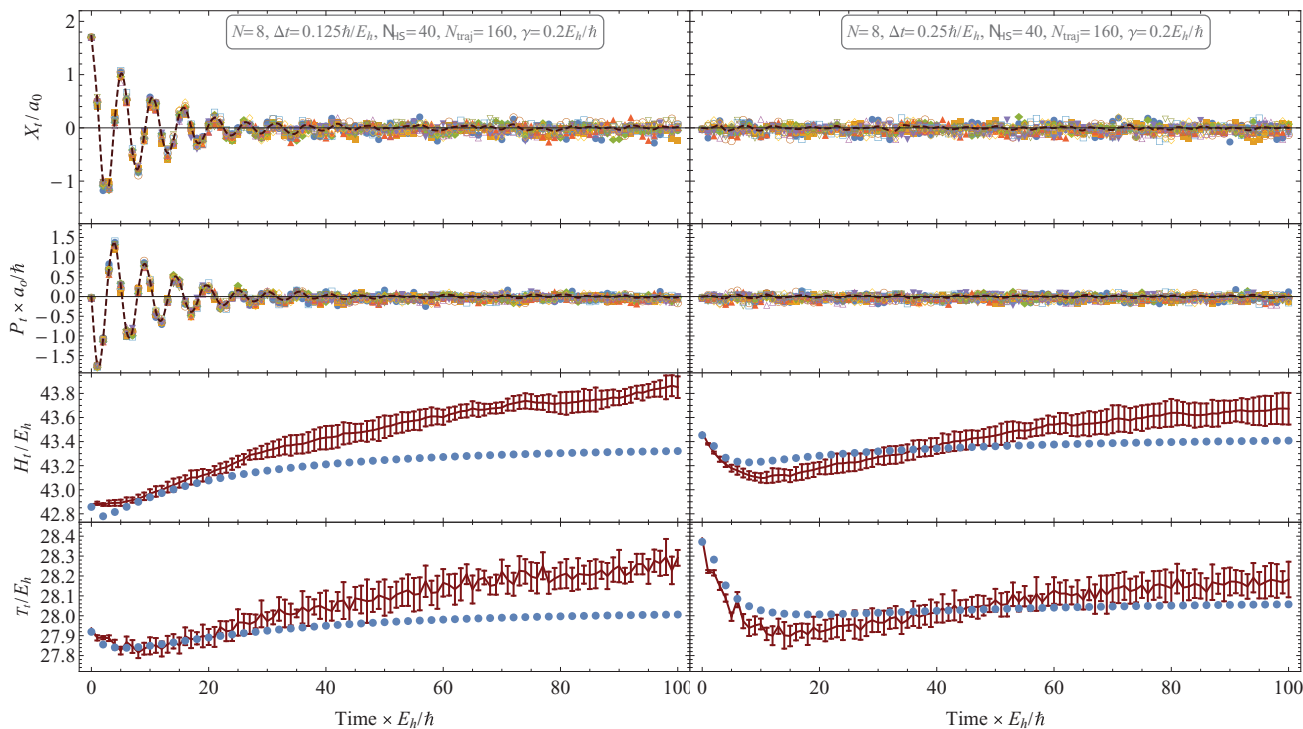


Figure 3. The time-dependent total displacement X_t , total momentum P_t , total energy H_t and total kinetic energy T_t transients for eight non-interacting Fermions in the double-well trap of Section 3.2, starting from a pure state $\hat{\rho}_\theta = |\Phi_\theta\rangle\langle\Phi_\theta|$ with $\theta = \pi/4$ (left panels) and $\theta = \pi/2$ (right panels). The X_t and P_t panels show as symbols the calculated results of 10 independent runs (each having 160 trajectories). The H_t and T_t results are depicted as statistical error bars centred on the average over the 10 runs and the dots are approximate transients computed from Equation (23).

for the sampling of the expected value of the Lindblad operator at a given time. Between different time-steps, a linear combination of K Slater wave functions, reproducing approximately the reduced DM of the system is formed (in this work we set $K = 1$). We have shown that this approach allows for accurate reconstruction of the dynamics of non-interacting Fermions in a Harmonic oscillator potential well, coupled to a bath through a specific Lindblad operator. We have also studied the dynamics of such Fermions in a double-well system, where a non-monotonic behaviour of the energy can be seen when starting from an excited eigenstate of the Hamiltonian.

This development has the potential of technically enabling a time-dependent density functional approach for electron dynamics in open systems. Future development is needed to assess the generality of the results presented here, implement the option of using a many determinant wave function (extending the method in this paper where we ‘collapse’ to a single determinant state after every time step) and apply the shifted contour technique for decreasing the HS statistical fluctuations [39,40]. Finally, the combination of the present development with stochastic orbital methods for electronic structure is an exciting venue [41–45].

Notes

1. This is true when the electrons interact with the bath through the one-body density matrix, which is the case of interest here and in most practical applications. There exists an important class of problems in which the electron interaction with the bath is ‘linear’ with the particle creation/destruction operators allowing an easier TDDFT adaption (see [21,25]).
2. This equation is obtained by first neglecting the off-diagonal elements of the DM (expressed as matrix in the eigenstate basis of the Hamiltonian), which leads to Pauli master equation [29] and then assuming that the populations in states i and j are uncorrelated.

Acknowledgments

This article is submitted to the Festschrift in honor of the pioneer of nonadiabatic dynamics Prof. Michael Baer. The second author, Roi Baer, hereby extends to his father a happy 80th birthday with deep love, appreciation and gratitude! Both authors gratefully thank the Israel Science Foundation Grant No. 189-14 for kindly funding this research.

Disclosure statement

No potential conflict of interest was reported by the authors.

Funding

Israel Science Foundation [grant number 189/14].

References

- [1] M. Head-Gordon and J.C. Tully, *J. Chem. Phys.* **103**, 10137–10145 (1995). doi:10.1063/1.469915
- [2] R.D. Schaller, J.M. Pietryga, S.V. Goupalov, M.A. Petruska, S.A. Ivanov, and V.I. Klimov, *Phys. Rev. Lett.* **95**, 196401 (2005). doi:10.1103/PhysRevLett.95.196401
- [3] M. Baer and G.D. Billing, editors, *The Role of Degenerate States in Chemistry*, Advances in Chemical Physics, **124 vols.** (Wiley-Interscience, New York, 2002). doi:10.1002/0471433462
- [4] M. Baer, *Beyond Born-Oppenheimer: Electronic Non-Adiabatic Coupling Terms and Conical Intersections* (Wiley, Hoboken, NJ, 2006), p. 234.
- [5] I. Gdor, A. Shapiro, C. Yang, D. Yanover, E. Lifshitz, and S. Ruhman, *ACS Nano* **9**, 2138–2147 (2015). doi:10.1021/nn5074868
- [6] N. Shenvi and J.C. Tully, *Faraday Discuss.* **157**, 325–335 (2012). doi:10.1039/c2fd20032e
- [7] S. Dong, D. Trivedi, S. Chakraborty, T. Kobayashi, Y. Chan, O.V. Prezhdo, and Z.-H. Loh, *Nano Lett.* **15**, 6875–6882 (2015). doi:10.1021/acs.nanolett.5b02786
- [8] E. Collini, C.Y. Wong, K.E. Wilk, P.M.G. Curmi, P. Brumer, and G.D. Scholes, *Nature* **463**, 644 (2010). doi:10.1038/nature08811
- [9] E. Romero, R. Augulis, V.I. Novoderezhkin, M. Ferretti, J. Thieme, D. Zigmantas, and R. Van Grondelle, *Nat. Phys.* **10**, 676 (2014). doi:10.1038/nphys3017
- [10] R.S. Ingarden, A. Kossakowski, and M. Ohya, *Information Dynamics and Open Systems: Classical and Quantum Approach*, **86 vols.** (Springer, Dordrecht, 2013).
- [11] M.A. Schlosshauer, *Decoherence: And the Quantum-to-Classical Transition* (Springer, Berlin, Heidelberg, 2007).
- [12] O.V. Prezhdo, *J. Chem. Phys.* **111**, 8366–8377 (1999). doi:10.1063/1.480178
- [13] L. Mühlbacher and E. Rabani, *Phys. Rev. Lett.* **100**, 176403 (2008). doi:10.1103/PhysRevLett.100.176403
- [14] D. Abramavicius, B. Palmieri, D.V. Voronine, F. Sanda, and S. Mukamel, *Chem. Rev.* **109**, 2350–2408 (2009). doi:10.1021/cr800268n
- [15] M. Esposito and M. Galperin, *Phys. Rev. B* **79**, 205303 (2009). doi:10.1103/PhysRevB.79.205303
- [16] E.Y. Wilner, H. Wang, G. Cohen, M. Thoss, and E. Rabani, *Phys. Rev. B* **88**, 045137 (2013). doi:10.1103/PhysRevB.88.045137
- [17] G. Cohen, E. Gull, D.R. Reichman, A.J. Millis, and E. Rabani, *Phys. Rev. B* **87**, 195108 (2013). doi:10.1103/PhysRevB.87.195108
- [18] C. Schinabeck, A. Erpenbeck, R. Härtle, and M. Thoss, *Phys. Rev. B* **94**, 201407 (2016). doi:10.1103/PhysRevB.94.201407
- [19] E. Runge and E.K.U. Gross, *Phys. Rev. Lett.* **52**, 997–1000 (1984). doi:10.1103/PhysRevLett.52.997
- [20] K. Burke, R. Car, and R. Gebauer, *Phys. Rev. Lett.* **94**, 146805 (2005).
- [21] S. Kurth, G. Stefanucci, C.O. Almbladh, A. Rubio, and E.K.U. Gross, *Phys. Rev. B* **72**, 035308 (2005). doi:10.1103/PhysRevB.72.035308
- [22] J.J. Zheng, Y. Zhao, and D.G. Truhlar, *J. Chem. Theory Comput.* **3**, 569–582 (2007). doi:10.1021/ct600281g
- [23] Y.V. Pershin, Y. Dubi, and M. Di Ventra, *Phys. Rev. B* **78**, 054302 (2008). doi:10.1103/PhysRevB.78.054302
- [24] J. Yuen-Zhou, D.G. Tempel, C.A. Rodríguez-Rosario, and A. Aspuru-Guzik, *Phys. Rev. Lett.* **104**, 043001 (2010). doi:10.1103/PhysRevLett.104.043001
- [25] O. Hod, C.A. Rodríguez-Rosario, T. Zelovich, and T. Frauenheim, *J. Phys. Chem. A* **120**, 3278–3285 (2016). doi:10.1021/acs.jpca.5b12212
- [26] G. Lindblad, *Commun. Math. Phys.* **48**, 119–130 (1976). doi:10.1007/BF01608499
- [27] V. Gorini, A. Kossakowski, and E.C.G. Sudarshan, *J. Math. Phys.* **17**, 821–825 (1976). doi:10.1063/1.522979
- [28] H.-P. Breuer and F. Petruccione, *The Theory of Open Quantum Systems* (Oxford University Press, Oxford, New York, 2002), p. 625.
- [29] G. Schaller, *Open Quantum Systems Far from Equilibrium*, **881 vols.** (Springer International Publishing, 2014). doi:10.1007/978-3-319-03877-3
- [30] R. Alicki and K. Lendi, *Quantum Dynamical Semigroups and Applications*, Lecture notes in Physics, **717 vols.** (Springer, Berlin, 2007), pp. 1–94. doi:10.1007/3-540-70861-8
- [31] H.J. Carmichael, *Phys. Rev. Lett.* **70**, 2273 (1993). doi:10.1103/PhysRevLett.70.2273
- [32] H.M. Wiseman and G.J. Milburn, *Phys. Rev. A* **47**, 642 (1993). doi:10.1103/PhysRevA.47.642
- [33] J. Dalibard, Y. Castin, and K. Mølmer, *Phys. Rev. Lett.* **68**, 580 (1992). doi:10.1103/PhysRevLett.68.580
- [34] N. Gisin and I.C. Percival, *J. Phys. A: Math. Gen.* **25**, 5677–5691 (1992). doi:10.1088/0305-4470/25/21/023
- [35] R.L. Stratonovich, *Dokl. Akad. Nauk SSSR* **115**, 1097 (1957).
- [36] J. Hubbard, *Phys. Rev. Lett.* **3**, 77 (1959). doi:10.1103/PhysRevLett.3.77
- [37] H. Tal-Ezer, *High Degree Interpolation Polynomial in Newton Form*, Tech. Rep. 88-39 (NASA (ICASE Report), 1988).
- [38] R. Kosloff, *Annu. Rev. Phys. Chem.* **45**, 145–178 (1994). doi:10.1146/annurev.pc.45.100194.001045
- [39] N. Rom, D.M. Charutz, and D. Neuhauser, *Chem. Phys. Lett.* **270**, 382–386 (1997). doi:10.1016/S0009-2614(97)00370-9
- [40] R. Baer, M.P. Head-Gordon, and D. Neuhauser, *J. Chem. Phys.* **109**, 6219–6226 (1998). doi:10.1063/1.477300
- [41] R. Baer, D. Neuhauser, and E. Rabani, *Phys. Rev. Lett.* **111**, 106402 (2013).
- [42] R. Baer and E. Rabani, *J. Chem. Phys.* **138**, 051102–4 (2013). doi:10.1063/1.4790600
- [43] Y. Cytter, E. Rabani, D. Neuhauser, and R. Baer, arXiv:1801.02163 [cond-mat.mtrl-sci] (2018).
- [44] E. Rabani, R. Baer, and D. Neuhauser, *Phys. Rev. B* **91**, 235302 (2015). doi:10.1103/PhysRevB.91.235302
- [45] D. Neuhauser, R. Baer, and D. Zgid, *J. Chem. Theory Comput.* **13**, 5396–5403 (2017). doi:10.1021/acs.jctc.7b00792